Simultaneous Excitation of Two Noninteracting Atoms with Time-Frequency Correlated Photon Pairs in a Superconducting Circuit

Wenhui Ren,[1,*] Wuxin Liu,[1,*] Chao Song,[1] Hekang Li,[1,2] Qiujiang Guo,[1] Zhen Wang,[1] Dongning Zheng,[2,3,†] Girish S. Agarwal,[4] Marlan O. Scully,[4,5] Shi-Yao Zhu,[1] H. Wang,[1,‡] and Da-Wei Wang[1,3,§]

[1]*Interdisciplinary Center for Quantum Information, State Key Laboratory of Modern Optical Instrumentation, and Zhejiang Province Key Laboratory of Quantum Technology and Device, Department of Physics, Zhejiang University, Hangzhou 310027, China*
[2]*Institute of Physics, Chinese Academy of Sciences, Bejing 100190, China*
[3]*CAS Center for Excellence in Topological Quantum Computation, University of Chinese Academy of Sciences, Bejing 100190, China*
[4]*Institute for Quantum Science and Engineering, Departments of Biological and Agricultural Engineering, Physics and Astronomy, Texas A&M University, College Station, Texas 77843, USA*
[5]*Baylor University, Waco, Texas 76706, USA*

(Received 8 April 2020; accepted 28 August 2020; published 21 September 2020)

We report the first observation of simultaneous excitation of two noninteracting atoms by a pair of time-frequency correlated photons in a superconducting circuit. The strong coupling regime of this process enables the synthesis of a three-body interaction Hamiltonian, which allows the generation of the tripartite Greenberger-Horne-Zeilinger state in a single step with a fidelity as high as 0.95. We further demonstrate the inhibition of the simultaneous two-atom excitation by continuously measuring whether the first photon is emitted. This work provides a new route in synthesizing many-body interaction Hamiltonian and coherent control of entanglement.

DOI: 10.1103/PhysRevLett.125.133601

Two-photon absorption, where two photons successively induce a quantum transition, was predicted by Goeppert-Mayer in 1931 [1]. It was not experimentally observed [2] until the invention of the laser, which provides the necessary intense monochromatic radiation. This effect has been widely used in fluorescent imaging [3,4], microfabrication [5], and quantum light sources [6]. It is worth noting that time-frequency entangled two photons or squeezed light can efficiently enhance two-photon absorption [7–10]. Two photons can also simultaneously excite two atoms that are interacting with each other [11–13], which offers new methods in collective control of quantum systems [14] and in spectroscopy with nanoscale resolution [15]. However, the requisite of interaction between atoms hinders the application of this effect in quantum information processing, since it is difficult to make far apart qubits interact with each other [16,17]. To circumvent this obstacle, many proposals [18–23] on simultaneous two-atom excitation have emerged. In particular, a single photon can simultaneously excite two atoms [18] with the effect of the counterrotating terms in ultrastrong coupling [24]. However, it is still challenging to realize the ultrastrong coupling and to mitigate its side effect. Until now, the simultaneous excitation of two noninteracting atoms has never been observed experimentally.

While two uncorrelated photons with frequencies ν_1 and ν_2 cannot simultaneously excite two noninteracting atoms with frequencies ω_1 and ω_2 at the two-photon resonance,

$$\nu_1 + \nu_2 = \omega_1 + \omega_2, \quad \nu_i \neq \omega_j \quad \text{for all } i, j = 1, 2, \tag{1}$$

it has been shown that the time-frequency entangled photon pairs generated in a cascade three-level system can excite two noninteracting atoms [10,25]. There are four quantum pathways for two atoms absorbing two photons, as shown in Fig. 1(a). With two independent photons, the probability amplitudes in these four pathways cancel out. However, if the two-photons are time-frequency entangled such that only two pathways are allowed, there is a finite probability that the two atoms are simultaneously excited. Unfortunately, the difficulty in collecting the photon pairs in free space greatly limits the efficiency of this process despite its promising applications in quantum spectroscopy [26,27]. In this Letter, we experimentally demonstrate that by confining the photon pairs in a cavity, two noninteracting artificial atoms can be simultaneously excited in a superconducting circuit. The three-body interaction between the light source and the two atoms is in the strong-coupling regime, such that the Greenberger-Horne-Zeilinger (GHZ) state [28] can be dynamically generated in a single step. We also show that this many-body dynamics can be coherently controlled by a continuous measurement [29–31]. This scheme requires neither counterrotating terms nor ultrastrong coupling and provides a new method

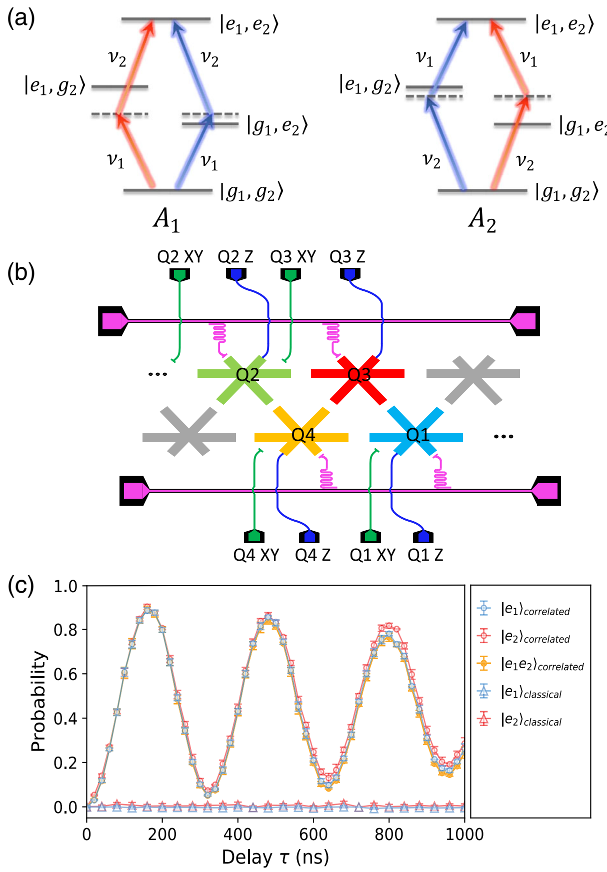

FIG. 1. Simultaneous excitation of two noninteracting qubits. (a) The quantum paths for A_1 and A_2 in Eq. (1). The pathways with the same color (blue or red) in A_1 and A_2 cancel each other, evident from their opposite values of the detunings from the atomic levels. (b) Sketch of part of the multiqubit superconducting circuit. Four qubits, labeled Q_1, Q_2, Q_3, and Q_4, are used in this experiment. Each qubit has its own flux bias line (blue) for fast frequency tuning and microwave line (green) for SU(2) spin rotations. For qubit readout, each qubit is capacitively coupled to its own readout resonator which is coupled to one of the two common transmission lines (pink). (c) The single-qubit probabilities of finding Q_1 (blue) and Q_2 (red) in their excited states when they are simultaneously driven by correlated photon pairs (circles) and uncorrelated classical microwaves (triangles) as functions of the interaction time τ. The joint probability of finding Q_1 and Q_2 in $|e_1, e_2\rangle$ by absorbing the correlated photon pairs is denoted by the filled yellow circles, which almost overlap with the empty blue and red circles. The simultaneous excitation of the two qubits is in conformity with the prediction of Ref. [10].

of synthesizing three-body interactions and entanglement generation.

Intuitively, it is easy to understand that two uncorrelated photons cannot simultaneously excite two noninteracting atoms under the condition in Eq. (1). Since each atom independently interacts with the two photons and can be considered separately, they cannot be excited because neither of them is in resonance with the photons. For the convenience of the discussion on the correlated photon pairs, we alternatively regard the two atoms as an entity and the transition probability can be calculated by considering which photon is absorbed first. The two-photon transition matrix element consists of two parts, A_1 and A_2, corresponding to the quantum pathways where ν_1 and ν_2 are first absorbed, as shown in Fig. 1(a). From the second order perturbation theory, we obtain [10],

$$A_1 = \frac{\kappa_{22}\kappa_{11}}{\nu_1 - \omega_1} + \frac{\kappa_{12}\kappa_{21}}{\nu_1 - \omega_2},$$
$$A_2 = \frac{\kappa_{21}\kappa_{12}}{\nu_2 - \omega_1} + \frac{\kappa_{11}\kappa_{22}}{\nu_2 - \omega_2}, \tag{2}$$

where κ_{ij} (much smaller than the one-photon detunings $|\nu_j - \omega_i|$ to avoid single-photon excitation and make second order process dominate) is the coupling strength between the atom and photon with frequencies ω_i and ν_j. The two-photon resonance in Eq. (1) renders that $A_1 = -A_2$ and the total two-photon transition matrix element is zero. However, if the two photons are correlated in such a way that some of the pathways are absent, we can remove the cancellation between the four pathways [32] (see [25] for more general discussion). A famous example is the time-frequency entangled photon pair generated from a cascade transition of a three-level atom [10], where the photon with frequency ν_1 is guaranteed to arrive at the atoms first. In this case only A_1 is present and it is generally nonzero. Consequently, the two atoms can be simultaneously excited. However, although time-frequency correlated photon pairs can be generated in nonlinear crystals [33] and atomic media [34], the simultaneous excitation of two noninteracting atoms has never been experimentally observed due to the difficulty both in finding the proper atoms and in collecting the entangled photon pairs.

Superconducting circuits offer a versatile platform to verify this interesting process, thanks to the flexibility of the artificial atoms (superconducting qubits) and the strong atom-photon coupling. The experiment is performed in a superconducting circuit consisting of multiple qubits interconnected in a zigzag triangular ladder [35] [see Fig. 1(b)], where the couplings between neighboring qubits are measured to be 10–13 MHz ($\times 2\pi$) and otherwise the couplings are weaker by about an order of magnitude. Each qubit is a frequency tunable transmon [36] circuit, whose sinusoidal potential well hosts multiple energy levels. The lowest three energy levels of the jth qubit Q_j are referred to as the ground state $|g_j\rangle$, the first excited state $|e_j\rangle$, and the second excited state $|f_j\rangle$, the latter of which is only involved in the experiment for Q_3. In our experimental setup, nonadjacent Q_1 and Q_2 are the two noninteracting atoms, and Q_3 is a qutrit that generates the cascade photon pairs. Q_4 is used as a measuring qubit in demonstrating the quantum Zeno effect. We can tune the resonance frequencies, perform SU(2) rotations and measure the quantum states of these qubits through their own flux bias lines, XY lines and readout resonators, respectively. At the experimental frequencies, the coherence performance of these qubits is characterized by the lifetime and Ramsey interference measurements, which yield the typical relaxation time $T_1 > 20\ \mu s$ and the Gaussian dephasing time $T_2^* \approx 1\ \mu s$ (see the Supplemental Material [37]).

The key experimental result is shown in Fig. 1(c). We first prepare Q_3 in the state $|f_3\rangle$, which subsequently emits two cascade photons with frequencies $\nu_1 \approx 2\pi \times 4.865$ GHz (for $|f_3\rangle \to |e_3\rangle$ transition) and $\nu_2 \approx 2\pi \times 5.100$ GHz (for $|e_3\rangle \to |g_3\rangle$ transition). These two photons simultaneously excite Q_1 and Q_2 with transition frequencies $\omega_1 \approx 2\pi \times 5.183$ GHz and $\omega_2 \approx 2\pi \times 4.781$ GHz, which satisfy Eq. (1). The strong coupling regime of this process is demonstrated by the well observed three-body Rabi oscillation in Fig. 1(c). We notice that the probability of finding Q_1 and Q_2 jointly in $|e_1, e_2\rangle$ (filled yellow circles) are almost the same as those of finding them individually excited (empty blue and red circles), which is evidence of the simultaneity of the two-atom excitation. In contrast, by simultaneously driving Q_1 and Q_2 with uncorrelated classical microwave pulses with the same frequencies ν_1 and ν_2, we observe no excitation of the qubits, as shown by the triangles in Fig. 1(c).

During the process of the simultaneous excitation of the two atoms, three-body entanglement between the light source and the two atoms is generated. This can be seen from the effective Hamiltonian between Q_1, Q_2, and Q_3 ($\hbar = 1$),

$$H_{\text{eff}} = A_1 \sigma_1^+ \sigma_2^+ \Xi_3^- + \text{H.c.}, \tag{3}$$

where A_1 is shown in Eq. (2) and its value is approximately $2\pi \times 2$ MHz. The raising operators for the three qubits are defined as $\sigma_j^+ = |e_j\rangle\langle g_j|$ for $j = 1$, 2 and $\Xi_3^+ = |f_3\rangle\langle g_3|$, and the lowering operators are their Hermitian conjugate. The Hamiltonian in Eq. (3) is a three-body interaction Hamiltonian that can entangle the three qubits in a single step [18,19,21], which has never been realized experimentally. In the present scheme, the large value of A_1 allows a high-fidelity GHZ state to be generated within a timescale much shorter than the typical coherence times of these qubits [37]. The experimental result is shown in Fig. 2.

The pulse sequence for generating the GHZ state is shown in Fig. 2(a). We first prepare Q_1-Q_2-Q_3 in the initial state $|\psi(0)\rangle = |g_1, g_2, f_3\rangle$ at their respective idle frequencies. Then the three qubits are quickly biased to their operating frequencies, so that Eq. (1) is satisfied [37]. After the dynamic evolution with a variable time τ, we bring the qubits back to their idle frequencies for measurement. The results of the joint measurement of the wave function $|\psi(\tau)\rangle = c_1(\tau)|g_1, g_2, f_3\rangle + c_2(\tau)|e_1, e_2, g_3\rangle$, ignoring the insignificant terms, are shown in Fig. 2(b), in which the experimentally obtained probabilities of $|c_1(\tau)|^2$ and $|c_2(\tau)|^2$ are plotted as functions of the interaction time τ. At $\tau \approx 88$ ns, ideally a three-qubit GHZ state $|\psi_{\text{GHZ}}\rangle = (|g_1, g_2, f_3\rangle + e^{i(\pi/2+\phi)}|e_1, e_2, g_3\rangle)/\sqrt{2}$ is generated, where ϕ is the dynamical phase picked up as the three qubits are tuned back to their idle frequencies right after the three-body dynamics. Quantum state tomography of a

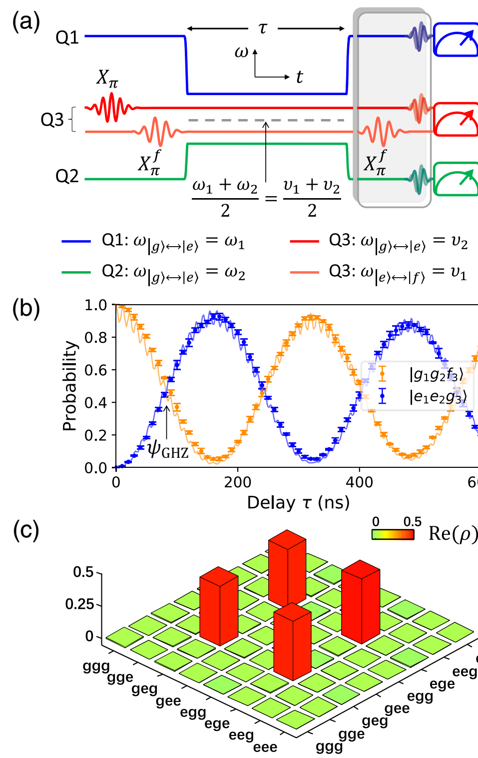

FIG. 2. Generating the GHZ state with the three-body interaction Hamiltonian. (a) Illustrative pulse sequence drawn in the frequency versus time frame. After initializing Q_1-Q_2-Q_3 in $|g_1, g_2, g_3\rangle$ at their respective idle frequencies, we prepare the state $|g_1, g_2, f_3\rangle$ by successively applying to Q_3 an X_π rotation (a π rotation around X axis transferring $|g_3\rangle$ to $|e_3\rangle$, red sinusoid) and an X_π^f rotation (transferring $|e_3\rangle$ to $|f_3\rangle$, light red sinusoid), following which we apply square pulses to tune the qubit frequencies, so that Eq. (1) is satisfied, for a dynamical evolution with a variable time τ. Finally we bring the qubits back to their idle frequencies for simultaneous readout: The same pulse sequence is repeated 1500 times to count the 12 probabilities $\{P_{ggg}, P_{gge}, P_{ggf} \cdots P_{gef}, P_{eef}\}$. The tomographic pulses in the shaded box is only inserted for QST of the GHZ state, $|\psi_{\text{GHZ}}\rangle$, where the X_π^f rotation transforms $|\psi_{\text{GHZ}}\rangle$ to its equivalent $|\psi'_{\text{GHZ}}\rangle = (|g_1, g_2, e_3\rangle + e^{i\phi}|e_1, e_2, g_3\rangle)/\sqrt{2}$, followed by null or $\pi/2$ rotations running through the Pauli set $\{I, X_{\pi/2}, Y_{\pi/2}\}$ for all three qubits. (b) The dominant occupational probabilities $|c_1(\tau)|^2$ for $|g_1, g_2, f_3\rangle$ (P_{ggf}, orange circles) and $|c_2(\tau)|^2$ for $|e_1, e_2, g_3\rangle$ (P_{eeg}, blue circles) measured as functions of the interaction time τ, in comparison with the numerical simulation (lines). (c) QST of the experimental $|\psi'_{\text{GHZ}}\rangle$ at $\tau \approx 88$ ns. Shown is the real part of the three-qubit density matrix, ρ, after a numerical rotation to remove the phase ϕ in $|\psi'_{\text{GHZ}}\rangle$.

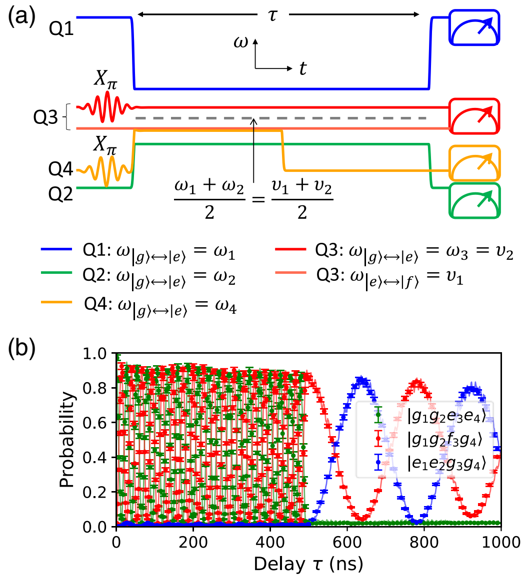

FIG. 3. The quantum Zeno effect of inhibiting the simultaneous two-atom excitation by continuous observation. (a) Illustrative pulse sequence drawn in the frequency versus time frame. Starting from all four qubits in their ground state, we first apply two X_π rotations to Q_3 and Q_4 (red and orange sinusoids). Then, we tune the frequencies of the four qubits into two-photon resonance, i.e., $\omega_1+\omega_2=\omega_3+\omega_4$ where $\omega_3=\nu_2$ and $\omega_4=\nu_1$, by applying square pulses to the qubit flux bias lines. At $\tau<500$ ns, Q_4 is continuously measuring the state of Q_3. At $\tau\approx 500$ ns when Q_3 is in state $|f_3\rangle$, we tune Q_4 to its idle frequency by applying a rectangle pulse. (b) The probabilities of finding the qubits in the state $|g_1,g_2,e_3,e_4\rangle$ (green circles), $|g_1,g_2,f_3,g_4\rangle$ (red circles), and $|e_1,e_2,g_3,g_4\rangle$ (blue circles) as functions of the interaction time τ, in comparison with the numerical simulation (lines). At $\tau<500$ ns, we observe the Rabi oscillation between $|g_1,g_2,e_3,e_4\rangle$ and $|g_1,g_2,f_3,g_4\rangle$, without the state $|e_1,e_2,g_3,g_4\rangle$ being noticeably excited due to the constant observation of Q_3 by Q_4. At $\tau>500$ ns when Q_4 is tuned off-resonant with Q_3, we observe the simultaneous excitation of Q_1 and Q_2 by the two cascade photons from Q_3.

ψ_{GHZ}-equivalent state is shown in Fig. 2(c), which has a state fidelity of 0.9491 ± 0.0073 [37]. The fidelity and preparation time of the GHZ state are comparable with those obtained via two-qubit gates [43].

Our superconducting circuit allows us to coherently control the simultaneous excitation of the two qubits by continuously measuring whether the first photon ν_1 is emitted. This is similar to the quantum Zeno effect [29–31,44–50], which was originally proposed as a fundamental question on whether frequent measurements can stop the spontaneous decay of a quantum system. The measurement is conducted by resonantly coupling qubit Q_4 to the transition $|f_3\rangle\leftrightarrow|e_3\rangle$ of Q_3, i.e., by setting $\omega_4\approx\nu_1$, so that Q_3 in $|f_3\rangle$ can excite Q_4 in about 14 ns, which is an order of magnitude shorter than the period of the three-body Rabi oscillation. By continuously observing Q_3, the three-body Rabi oscillation is totally inhibited, as shown in Fig. 3. In contrast, once the observation is stopped by tuning ω_4 far away from ν_1, the three-body Rabi oscillation appears.

The negligible simultaneous excitation of the two qubits Q_1 and Q_2 when being observed is reminiscent of the quantum Zeno effect, though as argued in literature especially in connection with the original experiment [30,51], the results of the experiment can be explained without invoking the wave function collapse [52,53]. We also notice that the state $|g_1,g_2,e_3,e_4\rangle$ has negligible coupling with $|e_1,e_2,g_3,g_4\rangle$, so that Q_4 does not have any direct effect on Q_1 and Q_2, which is ideal for measurement with a minimal impact on the observed system.

The simultaneous excitation of two noninteracting atoms is of fundamental importance to the basic law of physics. Since the two atoms are not required to have interactions, in principle they can be placed arbitrarily far apart [10]. This indicates that the law of energy conservation can be locally violated (the absence of the one-photon resonance), although the energy is still conserved globally (i.e., the two-photon resonance). This is achieved by breaking the symmetry in the arrival time of the two photons. Since local energy conservation originates from the time-translational symmetry according to the Noether's theorem, the asymmetric arrival time of the two photons relieves the constraint of the local energy conservation. This effect also offers new freedom in engineering many-body interaction Hamiltonians, complementing the two-body interaction Hamiltonians that have been intensively investigated and utilized in quantum simulation [54–57]. Following the same line, four-body and five-body interaction Hamiltonians can also be synthesized and the current multiqubit superconducting circuit can be used to demonstrate novel topological orders [58,59].

We acknowledge the support of the National Natural Science Foundation of China (Grants No. 11934011, No. 11725419, and No. 11874322), the National Key Research and Development Program of China (Grants No. 2019YFA0308100 and No. 2017YFA0304300), the Zhejiang Province Key Research and Development Program (Grant No. 2020C01019), Fundamental Research Funds for the Central Universities and the Strategic Priority Research Program of Chinese Academy of Sciences (Grant No. XDB28000000). We also gratefully acknowledge the support of AFOSR Award No. FA-9550-18-1-0141, ONR Award No. N00014-16-1-3054, and the Robert A. Welch Foundation (Awards No. A-1261 and No. A-1943) and the King Abdullah University of Science and Technology (KAUST) award. This research is also supported by King Abdulaziz City for Science and Technology (KACST).

*These authors contributed equally to this work.
†dzheng@iphy.ac.cn
‡hhwang@zju.edu.cn

[§]dwwang@zju.edu.cn

[1] M. Goeppert-Mayer, Ann. der Phys. **409**, 273 (1931).
[2] W. Kaiser and C. G. B. Garrett, Phys. Rev. Lett. **7**, 229 (1961).
[3] W. Denk, J. Strickler, and W. Webb, Science **248**, 73 (1990).
[4] P. T. C. So, C. Y. Dong, B. R. Masters, and K. M. Berland, Annu. Rev. Biomed. Eng. **2**, 399 (2000).
[5] S. Maruo, O. Nakamura, and S. Kawata, Opt. Lett. **22**, 132 (1997).
[6] Y.-M. He, H. Wang, C. Wang, M.-C. Chen, X. Ding, J. Qin, Z.-C. Duan, S. Chen, J.-P. Li, R.-Z. Liu, C. Schneider, M. Atatüre, S. Höfling, C.-Y. Lu, and J.-W. Pan, Nat. Phys. **15**, 941 (2019).
[7] J. Javanainen and P. L. Gould, Phys. Rev. A **41**, 5088 (1990).
[8] J. Gea-Banacloche, Phys. Rev. Lett. **62**, 1603 (1989).
[9] B. Dayan, A. Pe'er, A. A. Friesem, and Y. Silberberg, Phys. Rev. Lett. **94**, 043602 (2005).
[10] A. Muthukrishnan, G. S. Agarwal, and M. O. Scully, Phys. Rev. Lett. **93**, 093002 (2004).
[11] J. C. White, Opt. Lett. **6**, 242 (1981).
[12] G. V. Varada and G. S. Agarwal, Phys. Rev. A **45**, 6721 (1992).
[13] E. Pedrozo-Penafiel, R. R. Paiva, F. J. Vivanco, V. S. Bagnato, and K. M. Farias, Phys. Rev. Lett. **108**, 253004 (2012).
[14] F. Dell'Anno, S. De Siena, and F. Illuminati, Phys. Rep. **428**, 53 (2006).
[15] C. Hettich, C. Schmitt, J. Zitzmann, S. Kühn, I. Gerhardt, and V. Sandoghdar, Science **298**, 385 (2002).
[16] A. Bienfait, K. J. Satzinger, Y. P. Zhong, H.-S. Chang, M.-H. Chou, C. R. Conner1, É. Dumur, J. Grebel, G. A. Peairs, R. G. Povey, and A. N. Cleland, Science **364**, 368 (2019).
[17] P. Samutpraphoot, T. Dordevic, P. L. Ocola, H. Bernien, C. Senko, V. Vuletić, and M. D. Lukin, Phys. Rev. Lett. **124**, 063602 (2020).
[18] L. Garziano, V. Macrí, R. Stassi, O. Di Stefano, F. Nori, and S. Savasta, Phys. Rev. Lett. **117**, 043601 (2016).
[19] P. Zhao, X. Tan, H. Yu, S.-L. Zhu, and Y. Yu, Phys. Rev. A **96**, 043833 (2017).
[20] A. F. Kockum, A. Miranowicz, V. Macri, S. Savasta, and F. Nori, Phys. Rev. A **95**, 063849 (2017).
[21] R. Stassi, V. Macri, A. F. Kockum, O. Di Stefano, A. Miranowicz, S. Savasta, and F. Nori, Phys. Rev. A **96**, 023818 (2017).
[22] X. Liu, Q. Liao, G. Fang, and S. Liu, Sci. Rep. **9**, 2919 (2019).
[23] C. S. Munoz, A. F. Kockum, A. Miranowicz, and F. Nori, arXiv:1910.12875.
[24] A. F. Kockum, A. Miranowicz, S. De Liberato, S. Savasta, and F. Nori, Nat. Rev. Phys. **1**, 19 (2019).
[25] Z. Zheng, P. L. Saldanha, J. R. Rios Leite, and C. Fabre, Phys. Rev. A **88**, 033822 (2013).
[26] F. Schlawin, K. E. Dorfman, B. P. Fingerhut, and S. Mukamel, Nat. Commun. **4**, 1782 (2013).
[27] K. E. Dorfman, F. Schlawin, and S. Mukamel, Rev. Mod. Phys. **88**, 045008 (2016).
[28] D. M. Greenberger, M. A. Horne, A. Shimony, and A. Zeilinger, Am. J. Phys. **58**, 1131 (1990).
[29] B. Misra and E. C. G. Sudarshan, J. Math. Phys. (N.Y.) **18**, 756 (1977).
[30] W. M. Itano, D. J. Heinzen, J. J. Bollinger, and D. J. Wineland, Phys. Rev. A **41**, 2295 (1990).
[31] M. C. Fischer, B. Gutierrez-Medina, and M. G. Raizen, Phys. Rev. Lett. **87**, 040402 (2001).
[32] M. Richter and S. Mukamel, Phys. Rev. A **83**, 063805 (2011).
[33] T.-M. Zhao, H. Zhang, J. Yang, Z.-R. Sang, X. Jiang, X.-H. Bao, and J.-W. Pan, Phys. Rev. Lett. **112**, 103602 (2014).
[34] C. Liu, J. F. Chen, S. Zhang, S. Zhou, Y.-H. Kim, M. M. T. Loy, G. K. L. Wong, and S. Du, Phys. Rev. A **85**, 021803(R) (2012).
[35] W. Liu, W. Feng, W. Ren, D.-W. Wang, and H. Wang, Appl. Phys. Lett. **116**, 114001 (2020).
[36] J. Koch, T. M. Yu, J. Gambetta, A. A. Houck, D. I. Schuster, J. Majer, A. Blais, M. H. Devoret, S. M. Girvin, and R. J. Schoelkopf, Phys. Rev. A **76**, 042319 (2007).
[37] See the Supplemental Material at http://link.aps.org/supplemental/10.1103/PhysRevLett.125.133601 for the derivation of the effective Hamiltonian, characteristics of the quantum circuit, and data analysis on the experimental results, where Refs. [38–42] are cited.
[38] C. Cohen-Tannoudji, J. Dupont-Roc, and G. Grynberg, *Atom-Photon Interactions* (Wiley-VCH, New York, 1998).
[39] P. V. Klimov, J. Kelly, Z. Chen, M. Neeley, A. Megrant *et al.*, Phys. Rev. Lett. **121**, 090502 (2018).
[40] J. J. Burnett *et al.*, npj Quantum Inf. **5**, 54 (2019).
[41] Y. Zheng, C. Song, M. C. Chen, B. Xia, W. Liu *et al.*, Phys. Rev. Lett. **118**, 210504 (2017).
[42] H. K. Xu *et al.*, Nat. Commun. **7**, 11018 (2016).
[43] R. Barends *et al.*, Nature (London) **508**, 500 (2014).
[44] S. Maniscalco, F. Francica, R. L. Zaffino, N. Lo Gullo, and F. Plastina, Phys. Rev. Lett. **100**, 090503 (2008).
[45] P. Facchi, D. A. Lidar, and S. Pascazio, Phys. Rev. A **69**, 032314 (2004).
[46] Y. S. Patil, S. Chakram, and M. Vengalattore, Phys. Rev. Lett. **115**, 140402 (2015).
[47] A. Signoles, A. Facon, D. Grosso, I. Dotsenko, S. Haroche, J.-M. Raimond, M. Brune, and S. Gleyzes, Nat. Phys. **10**, 715 (2014).
[48] P. M. Harrington, J. T. Monroe, and K. W. Murch, Phys. Rev. Lett. **118**, 240401 (2017).
[49] C. Maier, T. Brydges, P. Jurcevic, N. Trautmann, C. Hempel, B. P. Lanyon, P. Hauke, R. Blatt, and C. F. Roos, Phys. Rev. Lett. **122**, 050501 (2019).
[50] S. Hacohen-Gourgy, L. P. Garcia-Pintos, L. S. Martin, J. Dressel, and I. Siddiqi, Phys. Rev. Lett. **120**, 020505 (2018).
[51] W. M. Itano, D. J. Heinzen, J. J. Bollinger, and D. J. Wineland, Phys. Rev. A **43**, 5168 (1991).
[52] L. E. Ballentine, Phys. Rev. A **43**, 5165 (1991).
[53] V. Frerichs and A. Schenzle, Phys. Rev. A **44**, 1962 (1991).
[54] D. F. James and J. Jerke, Can. J. Phys. **85**, 625 (2007).
[55] K. Xu, J.-J. Chen, Y. Zeng, Y.-R. Zhang, C. Song, W. Liu, Q. Guo, P. Zhang, D. Xu, H. Deng, K. Huang, H. Wang, X. Zhu, D. Zheng, and H. Fan, Phys. Rev. Lett. **120**, 050507 (2018).
[56] D.-W. Wang, C. Song, W. Feng, H. Cai, D. Xu, H. Deng, H. Li, D. Zheng, X. Zhu, H. Wang, S.-Y. Zhu, and M. O. Scully, Nat. Phys. **15**, 382 (2019).

[57] C. Song, K. Xu, H. Li, Y.-R. Zhang, X. Zhang, W. Liu, Q. Guo, Z. Wang, W. Ren, J. Hao, H. Feng, H. Fan, D. Zheng, D.-W. Wang, H. Wang, and S.-Y. Zhu, Science **365**, 574 (2019).
[58] H.-N. Dai, B. Yang, A. Reingruber, H. Sun, X.-F. Xu, Y.-A. Chen, Z.-S. Yuan, and J.-W. Pan, Nat. Phys. **13**, 1195 (2017).
[59] Z. Luo, J. Li, Z. Li, L.-Y. Hung, Y. Wan, X. Peng, and J. Du, Nat. Phys. **14**, 160 (2018).